Newtonian Jerky Dynamics and Inertial Instability

ZHONG Wei[1,2*] (钟 玮) and WU Rongsheng[1] (伍荣生)

1 *Key Laboratory of Mesoscale Severe Weather/Ministry of Education, and School of Atmospheric Sciences, Nanjing University, Nanjing* 210093

2 *Institute of Meteorology and Oceanography, PLA University of Science and Technology, Nanjing* 211101

(Received November 21, 2012; in final form March 11, 2013)

ABSTRACT

Newtonian jerky dynamics is applied to inertial instability analysis to study the nonlinear features of atmospheric motion under the action of variable forces. Theoretical analysis of the Newtonian jerky function is used to clarify the criteria for inertial instability, including the influences of the meridional distributions of absolute vorticity (ζ_g) and planetary vorticity (the β effect). The results indicate that the meridional structure of absolute vorticity plays a fundamental role in the dynamic features of inertial motion. Including only the β effect (with the assumption of constant ζ_g) does not change the instability criteria or the dynamic features of the flow, but combining the β effect with meridional variations of ζ_g introduces nonlinearities that significantly influence the instability criteria.

Numerical analysis is used to derive time series of position, velocity, and acceleration under different sets of parameters, as well as their trajectories in phase space. The time evolution of kinematic variables indicates that a regular wave-like change in acceleration corresponds to steady wave-like variations in position and velocity, while a rapid growth in acceleration (caused by a rapid intensification in the force acting on the parcel) corresponds to track shifts and abrupt changes in direction. Stable limiting cases under the f- and β-plane approximations yield periodic wave-like solutions, while unstable limiting cases yield exponential growth in all variables. Perturbing the value of absolute vorticity at the initial position (ζ_0) results in significant changes in the stability and dynamic features of the motion. Enhancement of the nonlinear term may cause chaotic behavior to emerge, suggesting a limit to the predictability of inertial motion.

Key words: Newtonian jerky dynamics, inertial instability, chaos

Citation: Zhong Wei and Wu Rongsheng, 2013: Newtonian jerky dynamics and inertial instability. *Acta Meteor. Sinica*, **27**(3), 400–414, doi: 10.1007/s13351-013-0311-8.

1. Introduction

The concepts of the distance, velocity (the first time derivative of distance), and acceleration (the second time derivative of distance) vectors are of paramount importance in understanding particle kinematics. Newton's second law formulates particle movements according to dynamical concepts such as force, momentum, and energy. The time derivative of acceleration (i.e., the third time derivative of distance), which is called jerk, attracted very little interest before the 1970s. Schot (1978) comprehensively reviewed the concept of jerk and its practical applications for designing intermittent-motion and transition curves.

Early dynamical research of jerk sometimes even misunderstood the concept. French (1971) concluded that the basic dynamics of an object influenced by a specified force had no relationship with second- or higher-order derivatives of velocity. However, Appell's equations of motion and the concept of acceleration energy that emerged at the end of the 20th century highlighted the importance of the dynamics of variable accelerated motion (Mei et al., 1991). Huang (1981) introduced jerk into the Chinese literature and proposed the concept of force variability, which connects jerk to the change of the force. In answer to the question "what is the simplest jerk function that gives

Supported by the National Natural Science Foundation of China (41275002 and 41175054) and Natural Science Key Foundation of China (41230421).

*Corresponding author: vivian.zhongwei@gmail.com.

chaos?" asked by Gottlieb (1996), Sprott (1997a) established the theory of jerky dynamics by transforming three first-order ordinary differential equations (ODEs) into a third-order, one-dimensional, autonomous ODE system, and promoted the application of this theory to chaos research. Linz (1997) investigated three restrictions on the jerk function to ensure that jerky dynamics can be derived from classical Newtonian equations, in the process formulating the Newtonian jerky dynamics (which expresses the explicit physical meaning of jerky motion).

It is well known that the forces acting on an air parcel change with time and space in atmospheric dynamics. A momentum equation with constant force is therefore unable to completely describe the complex evolution of the atmosphere. Sudden changes in weather systems are always associated with adjustments of the large-scale circulation and/or the redistribution of internal meteorological quantities in dynamics. These changes could equivalently be considered as the variability of external and/or internal forces in nature. The elementary equations of atmospheric motion can be regularly transformed into a second-order ODE of velocity, which is essentially a jerk equation. This analysis suggests that Newtonian jerky dynamics has promising applications in atmosphere science.

In this paper, we attempt to further understand the nonlinear aspects of atmospheric motion using Newtonian jerky dynamics. We propose this framework as an operative option for investigating the evolution of the atmosphere under the actions of variable forces. Inertial instability is one of the most important dynamical mechanisms in atmospheric science. This mechanism has been widely studied in the context of the genesis and development of weather systems (e.g. Emanuel, 1979, 1982). In Section 2, we review the definitions of the jerk function and Newtonian jerky dynamics, and then apply Newtonian jerky dynamics to the inertial motion. We obtain the criteria for inertial instability in the context of the meridional gradient of perturbation kinetic energy. We then present theoretical and numerical analyses of the nonlinear inertial motion equation and its instability criteria in Sections 3 and 4. The results are summarized in Section 5.

2. The jerk function and inertial motion equations

2.1 Definition of the jerk function

The jerk vector may be defined as

$$\boldsymbol{J} = \boldsymbol{a}' = \boldsymbol{V}'' = \boldsymbol{r}''', \tag{1}$$

where $\boldsymbol{a}(t)$, $\boldsymbol{V}(t)$, and $\boldsymbol{r}(t)$ are functions of time (t), and indicate the acceleration, velocity, and distance vectors, respectively. The prime denotes the time derivative d/dt. In general, the jerk motion can be determined by a scalar real ordinary differential equation that is (1) third-order, (2) explicit (i.e., linear in the highest derivative), and (3) autonomous (i.e., not explicitly dependent on time). This equation takes the form

$$\boldsymbol{r}''' = \boldsymbol{J}(\boldsymbol{r}, \boldsymbol{r}', \boldsymbol{r}''), \tag{2}$$

where $\boldsymbol{r}'$ and $\boldsymbol{r}''$ are the time derivative forms of velocity and acceleration, respectively, and $\boldsymbol{J}$ is the so-called jerky dynamics (Gottlieb, 1996). Sprott (1997b) formulated the general second-degree polynomial jerk function as

$$\begin{aligned}\boldsymbol{J} = {} & (\lambda_1 + \lambda_2\boldsymbol{r} + \lambda_3\boldsymbol{r}' + \lambda_4\boldsymbol{r}'')\boldsymbol{r}'' \\ & +(\lambda_5 + \lambda_6\boldsymbol{r} + \lambda_7\boldsymbol{r}')\boldsymbol{r}' + (\lambda_8 + \lambda_9\boldsymbol{r})\boldsymbol{r} + \lambda_{10}.\end{aligned} \tag{3}$$

The specific form of Eq. (3) is found by setting the coefficients λ_1–λ_{10} and identifying the dynamic characteristics of the solutions. These dynamic characteristics include motion under the action of variable forces and the possibility of chaos.

Not all jerky dynamics have explicit physical meaning. In the recognition, Linz (1997) defined Newtonian jerky dynamics as the subclass of all jerky dynamics that can be derived by taking the derivative of a one-dimensional Newtonian equation with respect to time (Linz, 1998). Newtonian jerky dynamics is related to the one-dimensional motion of a point particle of mass under the influence of an underlying force, and can be used to seek the physical relationships between the motion and the variability of the force. Additional restrictions of Newtonian jerky dynamics are discussed by Linz (1997). Given a particle of constant mass m acted upon by a complicated force vector $\boldsymbol{F}$, the total time derivative of the Newton equation can be written as

$$\boldsymbol{r}''' = \frac{1}{m}\frac{\mathrm{d}}{\mathrm{d}t}\boldsymbol{F} = \frac{1}{m}\left(\boldsymbol{r}'\frac{\partial \boldsymbol{F}}{\partial \boldsymbol{r}} + \boldsymbol{r}''\frac{\partial \boldsymbol{F}}{\partial \boldsymbol{r}'} + \frac{\partial \boldsymbol{F}}{\partial t}\right). \quad (4)$$

As discussed by Linz (1997), three criteria for relating the jerk function to an underlying force should be met: (1) the total and partial time derivatives of $\boldsymbol{F}$ cannot explicitly depend on time; (2) terms that are quadratic (or even more nonlinear) in $\boldsymbol{r}''$ cannot enter into the time-independent $\boldsymbol{J}$; and (3) Schwarz's theorem ($\frac{\partial^2 \boldsymbol{F}}{\partial \boldsymbol{r}\partial \boldsymbol{r}'} = \frac{\partial^2 \boldsymbol{F}}{\partial \boldsymbol{r}'\partial \boldsymbol{r}}$) must be satisfied to ensure the integrability of $\boldsymbol{J}$. Linz (1997) also examined several famous nonlinear models, including the well-known Lorenz model (Lorenz, 1963) based on the simplified form of the convection equations derived by Saltzman (1962).

The original form of the model proposed by Lorenz (1963) is

$$x' = -\sigma x + \sigma y, \quad (5a)$$

$$y' = -xz + \tau x - y, \quad (5b)$$

$$z' = xy - bz, \quad (5c)$$

with σ, τ, and b representing control parameters. The jerk function can be obtained by the elimination method as

$$\begin{aligned} x''' = \boldsymbol{J} = &-\left[(\sigma + b + 1) - (\ln x)'\right] x'' \\ &- \left[b(\sigma+1) + x^2 - (\sigma+1)(\ln x)'\right] x' \\ &+ \left[\sigma b(\tau - 1) - \sigma x^2\right] x. \end{aligned} \quad (6)$$

Comparing Eq. (6) to Eq. (4), we find that the jerk function does not explicitly depend on time, and therefore fulfills criterion (1) above. However, Eq. (6) satisfies neither criterion (2) nor criterion (3) due to the presence of the logarithmic derivatives $(\ln x)'$ and the inequality between $\frac{\partial^2 \boldsymbol{F}}{\partial \boldsymbol{r}\partial \boldsymbol{r}'}$ and $\frac{\partial^2 \boldsymbol{F}}{\partial \boldsymbol{r}'\partial \boldsymbol{r}}$. This analysis shows that the Lorenz model is not Newtonian jerky.

2.2 Equations for inertial motion

Inertial motion and its instability were first investigated by Rayleigh (1916), who discussed atmospheric motion under the co-action of the pressure gradient and Coriolis forces. The results of these fundamental investigations have been widely used to explain the genesis and enhancement of convection (e.g., Tomas and Webster, 1997), the development of tropical cyclones (e.g., Schubert and Hack, 1982), and the formation of secondary eyewalls (e.g., Rozoff et al., 2012). The governing equations of inertial motion are fundamentally nonlinear, but most current tools for dynamic analysis still rely on linearization. In this section, we apply Newtonian jerky dynamics to the two-dimensional equations of inertial motion to further our understanding of nonlinear atmospheric dynamics.

We assume that the basic flow is directed in the zonal direction, fulfills geostrophic balance, and is constant with time. These assumptions mean that the geostrophic velocity (u_{g}, v_{g}) and geopotential height (Φ) satisfy the equations $u_{\mathrm{g}} = \frac{1}{f}\frac{\partial \Phi}{\partial x}$, $v_{\mathrm{g}} = 0$, and $\frac{\partial u_{\mathrm{g}}}{\partial t} = 0$, where f is the Coriolis parameter (often taken as a constant f_0 under the f-plane approximation). The equations of two-dimensional motion for a parcel in this flow are

$$\frac{\mathrm{d}u}{\mathrm{d}t} - fv = 0, \quad (7a)$$

$$\frac{\mathrm{d}v}{\mathrm{d}t} + f(u - u_{\mathrm{g}}) = 0. \quad (7b)$$

As discussed by Dutton (1995), u and v represent the zonal and meridional velocity, respectively. A northward displacement δy from an initial position y_0 will increase the eastward speed from its initial value of $u_{\mathrm{g}}(y_0)$. Under a linear approximation, the eastward speed of the parcel at $y_0 + \delta y$ is $u = u_{\mathrm{g}}(y_0) + f\delta y$. Furthermore, $u_{\mathrm{g}} = u_{\mathrm{g}}(y_0) + \delta y\frac{\partial u_{\mathrm{g}}}{\partial y}$. Equation (7b) can then be written as

$$\frac{\mathrm{d}v}{\mathrm{d}t} = \frac{\mathrm{d}^2 y}{\mathrm{d}t^2} = -f\zeta_{\mathrm{g}}\delta y, \quad (8)$$

where $\zeta_{\mathrm{g}} = f - \partial u_{\mathrm{g}}/\partial y$ is the vertical component of the geostrophic absolute vorticity. For an initial perturbation $v_0 > 0$, the movement of the parcel at $y_0 + \delta y$ can be classified into three categories based on the value of ζ_{g}: (1) unstable motion ($\mathrm{d}v/\mathrm{d}t > 0$ with negative ζ_{g}); (2) stable oscillations ($\mathrm{d}v/\mathrm{d}t < 0$ with positive ζ_{g}); and (3) neutral states ($\zeta_{\mathrm{g}} = 0$ and $\mathrm{d}v/\mathrm{d}t = 0$). The same results are obtained for a southward displacement. This is classical dynamical analysis of inertial instability; however, this simple approach is only valid with the linear approximation near y_0 and the assumption that $-f\zeta_g$ is constant in Eq. (8). Here, we employ Newtonian jerky dynamics to investigate the more general case with complicated spatial structures of absolute vorticity and/or significant displacements in latitudes.

The kinematic meridional velocity and acceleration can be defined as $y' = v$, $y'' = \mathrm{d}v/\mathrm{d}t = a$. Substitution into Eqs. (7a) and (7b) yields the jerky function for inertial motion.

$$y''' = \gamma y'y'' + \mu y'. \tag{9}$$

Two control parameters appear in Eq. (9). The parameter $\gamma = \beta/f$ is the ratio of the meridional gradient of planetary vorticity to the value of planetary vorticity, and can be thought of as representing the influence of the curvature of the earth on the inertial motion. Two approximations may be made to simplify the treatment: $\gamma = 0$ (the f-plane approximation), or $\gamma = \beta/f_0$, in which both β ($= 10^{-11}$ m^{-1} s^{-1}) and f_0 ($= 10^{-5}$ s^{-1}) are set to be constants (the β-plane approximation). The parameter $\mu = f(\partial u_g/\partial y - f) = -f\zeta_g$ represents the structure of the vertical component of geostrophic absolute vorticity, which reflects the structure of the underlying flow. Classical analysis of inertial motion typically assumes that μ is constant. Here, we analyze the conditions for inertial instability associated with more complicated meridional distributions of ζ_g. Under the f- or β-plane approximation, this parameter can be simplified to $\mu = -f_0\zeta_g$. The dynamical features of Eq. (9) depend strongly on the control parameters γ and μ, or more specifically the meridional variability of planetary and absolute vorticity. Equation (9) satisfies the three criteria outlined by Linz (1997). This jerk function, which is derived directly from the atmospheric momentum equation, is therefore Newtonian jerky.

In typical classical analyses of inertial motion, the initial conditions for the distance, velocity, and acceleration of the parcel satisfy

$$\begin{cases} y|_{t=0} = 0, \\ y'|_{t=0} = v_0, \\ y''|_{t=0} = 0. \end{cases} \tag{10}$$

Since the acceleration $y'' = (\mathrm{d}/\mathrm{d}y)(y'^2/2)$, the jerk $y''' = y'(\mathrm{d}^2/\mathrm{d}y^2)(y'^2/2)$. Given the additional condition that $y' \neq 0$, the jerky function of Eq. (9) can be written as

$$\frac{\mathrm{d}^2E}{\mathrm{d}y^2} - \gamma\frac{\mathrm{d}E}{\mathrm{d}y} - \mu = 0, \tag{11}$$

where $E = y'^2/2$ is the zonal perturbation kinetic energy. The Newtonian jerky dynamics of inertial motion in the form of a third-order ODE that depends on time is thereby transformed into a second-order ODE of the zonal perturbation kinetic energy equation that depends on position. We can then modify Eq. (10) to derive suitable initial conditions for Eq. (11):

$$\begin{cases} y|_{t=0} = 0, \\ E|_{y=0} = v_0^2/2, \\ (\mathrm{d}E/\mathrm{d}y)|_{y=0} = y''|_{y=0} = 0. \end{cases} \tag{12}$$

The criteria $y'' = \mathrm{d}v/\mathrm{d}t$ for estimating the instability of inertial motion then takes the equivalent form $y'' = \mathrm{d}E/\mathrm{d}y$ in Eq. (11). This means that the sign of $\mathrm{d}E/\mathrm{d}y$ determines the stability of the inertial motion. If $\mathrm{d}E/\mathrm{d}y > 0$, the zonal perturbation kinetic energy increases with meridional distance; the parcel is then unstable and accelerates away from its initial position. By contrast, if $\mathrm{d}E/\mathrm{d}y < 0$, the parcel is stable and oscillates around its initial position. The key to obtaining the dynamic features of the general equations of inertial motion is therefore to seek the solution of $\mathrm{d}E/\mathrm{d}y$ under different sets of control parameters.

3. Theoretical analysis

The simplified Newtonian jerky equation of zonal perturbation kinetic energy enables us to solve Eq. (11) theoretically. In this section, we use this approach to gain further insight into inertial stability under more complicated control parameter regimes.

3.1 Inertial motion under the f-plane approximation

Under the f-plane approximation, $\gamma = 0$ and Eqs. (9) and (11) can be simplified as

$$y''' = \mu y', \tag{13a}$$

$$\frac{\mathrm{d}^2E}{\mathrm{d}y^2} = \mu. \tag{13b}$$

Equation (13) is linear if μ is a constant, yielding the criterion $y'' = \dfrac{\mathrm{d}E}{\mathrm{d}y} = \mu y + \dfrac{v_0^2}{2}$. We follow the classical analysis by assuming that the initial perturbation in the meridional direction y is positive (northward). The stability of the system is then determined solely by the sign of μ (an initial southward perturbation yields the same result). This result is identical to that obtained from classical analysis of inertial instability: the system is stable when the absolute vorticity is negative (positive μ) and unstable when the absolute vorticity is positive (negative μ).

The dynamic features of this system change when μ is defined as a function of y. We define μ as a quadratic polynomial with the form $\mu = c_0 + c_1 y + c_2 y^2$ for simplicity, where c_0, c_1, and c_2 are constants. Although Eq. (13b) still retains its linear features, Eq. (13a) has nonlinear terms when one (or both) of c_1 and c_2 is (are) non-zero. The meridional distribution of the absolute vorticity is determined by the choices for c_0, c_1, and c_2. If c_1 and/or c_2 are/is non-zero, the meridional gradient in the absolute vorticity is non-zero and analogous to the β effect (Montgomery and Kallenbach, 1997). This difference leads to significant changes in the dynamic behavior of the system.

For the sake of discussion, we define some of the parameters of the ambient flow based on the relationship between μ and ζ_g. Specifically, we define the meridional gradient of absolute vorticity $\zeta_y = \mathrm{d}\zeta_\mathrm{g}/\mathrm{d}y$ as $-\mathrm{d}\mu/(f_0\mathrm{d}y)$, the second-order derivative of absolute vorticity $\zeta_{yy} = \mathrm{d}^2\zeta_\mathrm{g}/\mathrm{d}y^2$ as $-\mathrm{d}^2\mu/(f_0\mathrm{d}y^2)$, the absolute vorticity at the initial position $\zeta_0 = \zeta_\mathrm{g}|_{y=0}$ as $-(\mu/f_0)|_{y=0}$, and the meridional gradient of the initial absolute vorticity ζ_{y0} as $-(\mathrm{d}\mu/f_0\mathrm{d}y)|_{y=0}$. The constants c_0, c_1, and c_2 are given by

$$\begin{cases} c_0 = -f_0\zeta_0, \\ c_1 = -f_0\zeta_{y0}, \\ c_2 = -f_0\zeta_{yy}/2. \end{cases} \tag{14}$$

Substituting from Eqs. (14) and (12), the theoretical solutions of Eq. (13b) are

$$E = -f_0\left(\frac{\zeta_{yy}}{24}y^4 + \frac{\zeta_{y0}}{6}y^3 + \frac{\zeta_0}{2}y^2 + \frac{v_0^2}{2}\right), \tag{15a}$$

$$\frac{\mathrm{d}E}{\mathrm{d}y} = -\frac{f_0 y}{2}\left(\frac{\zeta_{yy}}{3}y^2 + \zeta_{y0}y + 2\zeta_0\right). \tag{15b}$$

Equation (15a) indicates that the system state is determined not only by the structure of the ambient flow (ζ_{yy}, ζ_{y0}, and ζ_0), but also by the meridional displacement y. Table 1 lists the criteria for inertial instability associated with various configurations of the flow parameters. If the meridional displacement y is assumed to be positive, then two limiting cases are obtained that are qualitatively independent of y. The first case is that all of the flow parameters are positive ($\zeta_{yy} > 0$, $\zeta_{y0} > 0$, and $\zeta_0 > 0$). This case results in stable motion ($\mathrm{d}E/\mathrm{d}y < 0$). In other words, if the (quadratic) absolute vorticity has a minimum, and the absolute vorticity and its gradient are positive at the initial position, then the motion is inertially stable. The second case is that all of the flow parameters are negative ($\zeta_{yy} < 0$, $\zeta_{y0} < 0$, and $\zeta_0 < 0$). This case results in unstable motion, meaning that the parcel would accelerate away from its initial position. Outside of these two limiting cases, the dynamic features are uncertain. All three parameters are determined by the distribution of ζ_g, with ζ_{yy} and ζ_{y0} dependent on the shape of the distribution and ζ_0 simply the value of ζ_g at the initial position. The simplest approach is to retain the shape of ζ_g and change the sign of ζ_0. In this case, $\mathrm{d}E/\mathrm{d}y$ may change sign as y varies. In Section 4, we perform numerical calculations to show the uncertainty in this condition.

We primarily consider cases for which the flow parameters are non-zero, as these represent the most common situation. If one or more of the flow parameters are zero, the distribution of absolute vorticity becomes monotonic or constant. These cases can be considered by setting the relevant parameters to zero.

Table 1. Criteria for inertial instability under the f-plane approximation

	Stable case ($\mathrm{d}E/\mathrm{d}y < 0$)	Unstable case ($\mathrm{d}E/\mathrm{d}y > 0$)	Uncertain case (only considering the effects of ζ_0)		
ζ_{yy}	$\zeta_{yy} > 0$	$\zeta_{yy} < 0$	$\zeta_{yy} > 0$		$\zeta_{yy} < 0$
ζ_{y0}	$\zeta_{y0} > 0$	$\zeta_{y0} < 0$	$\zeta_{y0} > 0$	or	$\zeta_{y0} < 0$
ζ_0	$\zeta_0 > 0$	$\zeta_0 < 0$	$\zeta_0 < 0$		$\zeta_0 > 0$

Taking the meridional structure of $\zeta_{\rm g}$ into consideration, Eq. (13a) can be rewritten as

$$y''' = c_0 y' + c_1 y y' + c_2 y^2 y'. \tag{16}$$

Equation (16) may then be compared with the simplest chaotic dissipative system described by Sprott (1997b). Although no y'' term appears on the right hand side of Eq. (16), the nonlinear terms yy' and y^2y' may generate chaos. The form of the solution is determined by the parameters c_0, c_1, and c_2, which correspond to the physical atmospheric parameters ζ_{yy}, ζ_{y0}, and ζ_0.

The expression of E in Eq. (15a) indicates that the paths in the $y'-y$ phase plane are closed oval-type curves:

$$y' = \pm\sqrt{-f_0\left(\frac{\zeta_{yy}}{12}y^4 + \frac{\zeta_{y0}}{3}y^3 + \zeta_0 y^2 + v_0^2\right)}. \tag{17}$$

The solution $y(t)$ is then obtained implicitly as an inverse function through the quadrature (omitted here), and the time period of the motion is

$$t = \pm f_0^{-1/2}\int_{y_0}^{y}\left(-\frac{\zeta_{yy}}{12}y^4 - \frac{\zeta_{y0}}{3}y^3 - \zeta_0 y^2 - v_0^2\right)^{-1/2}{\rm d}y. \tag{18}$$

We can use Eq. (18) to investigate whether the phase plane plots yielded by this system (Sprott, 1997b) are period-1 (limit cycle) orbits, period-doubling orbits, or chaotic orbits. The results of this investigation are presented in Section 4.

3.2 Inertial motion under the β-plane approximation

Changes in the Coriolis parameter must be taken into account if the parcel is displaced a significant distance. In this case, we should employ the β-plane approximation with a non-zero constant γ in Eqs. (9) and (11).

To recover the nonlinear term $\gamma y' y''$, we start with the simple ambient flow described by a constant μ. The theoretical solutions of Eqs. (11) and (12) are

$$E = \frac{\mu}{\gamma^2}{\rm e}^{\gamma y} - \frac{\mu}{\gamma}y + \frac{\gamma^2 v_0^2 - 2\mu}{2\gamma^2}, \tag{19a}$$

$$\frac{{\rm d}E}{{\rm d}y} = \frac{\mu}{\gamma}({\rm e}^{\gamma y} - 1). \tag{19b}$$

Usually $\gamma = \beta/f_0 > 0$ and $({\rm e}^{\gamma y} - 1) > 0$, in which case the sign of ${\rm d}E/{\rm d}y$ is determined solely by the sign of μ as in the classical inertial instability analysis discussed above. Furthermore, if both control parameters (μ and γ) are constants, the jerk function depends only on y' and y''. This jerk function can then be written as a second-order autonomous ODE in y', and cannot exhibit chaos (Gottlieb, 1998).

The theoretical solutions of Eq. (11) for the more complex ambient flow with $\mu = c_0 + c_1 y + c_2 y^2$ (with the constants set as in Eq. (14)) are

$$\begin{aligned}E = &-\frac{v_0^2}{2} - \frac{f_0}{\gamma^4}(\zeta_{yy} + \gamma\zeta_{y0} + \gamma^2\zeta_0){\rm e}^{\gamma y}\\ &+\frac{f_0}{6\gamma}(y^3\zeta_{yy} + 3y^2\zeta_{y0} + 6y\zeta_0)\\ &+\frac{f_0}{\gamma^2}\left(\frac{\zeta_{yy}}{2}y^2 + y\zeta_{y0} + \zeta_0\right)\\ &+\frac{f_0}{\gamma^3}(y\zeta_{yy} + \zeta_{y0}) + \frac{f_0}{\gamma^4}\zeta_{yy},\end{aligned} \tag{20a}$$

$$\begin{aligned}\frac{{\rm d}E}{{\rm d}y} = \frac{f_0}{\gamma^3}\Big[&\frac{\zeta_{yy}}{2}\gamma^2 y^2 + (\zeta_{yy} + \gamma\zeta_{y0})\gamma y\\ &+(\zeta_{yy} + \gamma\zeta_{y0} + \gamma^2\zeta_0)(1 - {\rm e}^{\gamma y})\Big],\end{aligned} \tag{20b}$$

where $(1 - {\rm e}^{\gamma y}) < 0$. The criteria for instability according to Eq. (20a) are listed in Table 2. A stable limiting case results when $\zeta_{yy} < 0$, $\zeta_{y0} \leqslant -\zeta_{yy}/\gamma$, and $\zeta_0 \geqslant -(\gamma\zeta_{y0} + \zeta_{yy})/\gamma^2$. These three conditions are equivalent to (1) the (quadratic) absolute vorticity has a maximum in the direction of the initial displacement, (2) the meridional gradient of the absolute vorticity is less than $|\zeta_{yy}|/\gamma$, and (3) the absolute vorticity at the initial position is positive and greater than $|\gamma\zeta_{y0} + \zeta_{yy}|/\gamma^2$. An unstable limiting case results when none of these three conditions is met. The stability or instability of all other cases depends not only on the structure of the ambient flow, but also on the meridional displacement y. In Section 4, we provide numerical results for cases in which the shape of the absolute vorticity distribution is retained while the sign of ζ_0 is changing.

The preceding analysis indicates that inclusion or exclusion of the β effect does not affect the stability or dynamic features of inertial motion if the absolute

Table 2. Criteria for inertial instability under the β-plane approximation

	Stable case ($\mathrm{d}E/\mathrm{d}y$ <0)	Unstable case ($\mathrm{d}E/\mathrm{d}y$ >0)	Uncertain case (only considering the effects of ζ_0)		
ζ_{yy}	$\zeta_{yy}<0$	$\zeta_{yy}>0$	$\zeta_{yy}<0$		$\zeta_{yy}>0$
ζ_{y0}	$\zeta_{y0}\leqslant-\zeta_{yy}/\gamma$	$\zeta_{y0}\geqslant-\zeta_{yy}/\gamma$	$\zeta_{y0}\leqslant-\zeta_{yy}/\gamma$	or	$\zeta_{y0}\geqslant-\zeta_{yy}/\gamma$
ζ_0	$\zeta_0\geqslant-(\gamma\zeta_{y0}+\zeta_{yy})/\gamma^2$	$\zeta_0\leqslant-(\gamma\zeta_{y0}+\zeta_{yy})/\gamma^2$	$\zeta_0\leqslant-(\gamma\zeta_{y0}+\zeta_{yy})/\gamma^2$		$\zeta_0\geqslant-(\gamma\zeta_{y0}+\zeta_{yy})/\gamma^2$

vorticity distribution is constant; however, the nonlinear term $\gamma y'y''$ exerts a significant influence on the stability criteria if the absolute vorticity varies in the meridional direction. Figure 1 shows the meridional profiles of ζ_{g} in stable and unstable cases under the f- and β-plane approximations. Under the f-plane approximation, if ζ_{g} increases with a meridional displacement from a positive initial value, the system is inertially stable. By contrast, the system is inertially unstable if ζ_{g} decreases with a meridional displacement from a negative initial value. Under the β-plane approximation, the ζ_{yy} criterion for stability (or instability) changes signs. The criteria for ζ_{y0} and ζ_0 are more complicated, with threshold values that depend on the parameters ζ_{yy}, ζ_{y0}, and γ. The requirements for the stable and unstable limiting cases are quite strict. Violation of any of the requirements shown in Fig. 1 (or listed in Tables 1 and 2) leads to uncertainty in the inertial stability of the system. This uncertainty is analyzed numerically in the next section.

4. Numerical results

In this section, we calculate numerical solutions to the Newtonian jerky equations that complement the theoretical discussion in Section 3. The kinematic definitions of the perturbation meridional velocity (v) and acceleration (a) enable them to be expressed as $\mathrm{d}y/\mathrm{d}t$ and $\mathrm{d}^2y/\mathrm{d}t^2$, respectively. The 3rd-order ODE for the solitary variable y (Eq. (9)) can be converted to a group of closed ODEs for y, v, and a:

$$\frac{\mathrm{d}y}{\mathrm{d}t}=v,\ \frac{\mathrm{d}^2y}{\mathrm{d}t^2}=a,\ \frac{\mathrm{d}^3y}{\mathrm{d}t^3}=\gamma va+\mu v, \tag{21}$$

The parameter γ is set to either 0 (under the f-plane approximation) or a constant β/f_0 (under the β-plane approximation). As in Section 3, the parameter μ is defined as a second-order polynomial in y. This ensures that the equation of inertial motion is nonlinear even under the f-plane approximation. The numerical results are obtained using the Matlab$^{\mathrm{TM}}$ function

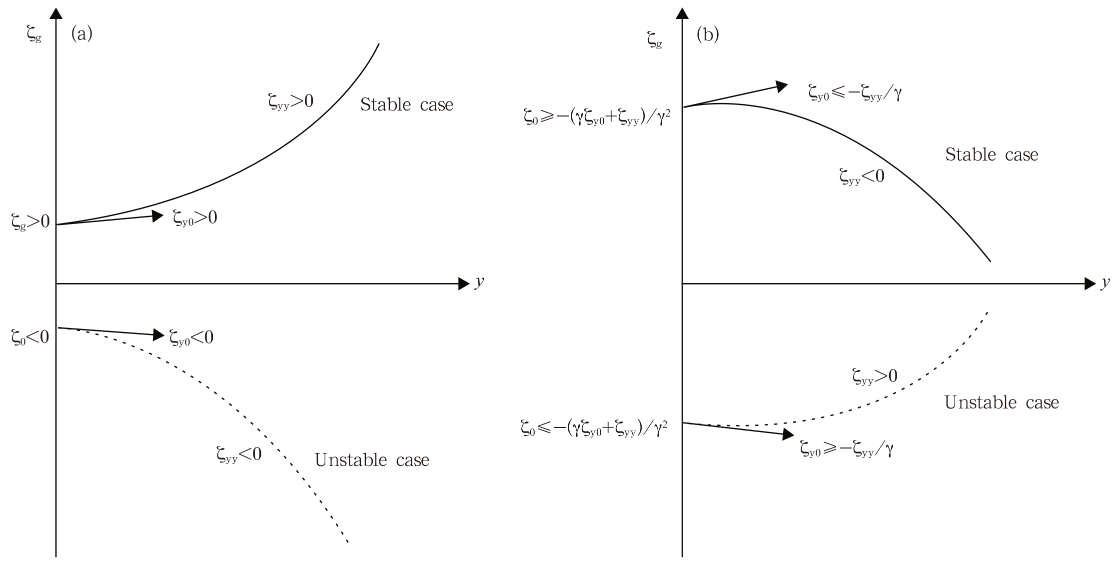

Fig. 1. A sketch of the absolute vorticity (ζ_{g}) with meridional displacement (y) in the stable (solid line) and unstable (dashed line) cases under (a) the f-plane approximation and (b) the β-plane approximation.

ode45. The ordinary atmospheric momentum equations based on Newton's second law consist of only two equations: a kinematic equation defining the velocity and a dynamic equation describing the rate of change in this velocity under the influence of forces. This system cannot produce chaos because it only includes a two-dimensional phase space (Sprott, 1997b). Gottlieb (1996) pointed out that Newtonian jerky dynamics provides a topological geometric foundation for establishing the relationship between chaotic motion and variable forces.

We have designed eight numerical experiments to test the stability of the flow under different sets of parameters. The values of the parameters for each experiment are listed in Tables 3 and 4. The planetary vorticity and its meridional gradient are approximated as $f_0 = 10^{-5}$ s^{-1} and $\beta = 10^{-11}$ m^{-1} s^{-1} ($\beta = 0$ under the f-plane approximation). We use the initial conditions set out in Eq. (10) and prescribe an initial northward perturbation velocity (v_0) of 1 m s^{-1} at the initial position $y_0 = 0$. We use the criteria for the β-plane approximation to calculate the threshold values for the parameters ζ_{y0} and ζ_0 (Table 4).

The f-plane approximation is appropriate for mesoscale or smaller scale atmospheric motions. The parameter values listed in Table 3 are therefore specified to ensure an apparent and reasonable change in ζ_g within 200 km (Figs. 2a and 3a). The ambient flow, instability criteria, and time series of perturbations in the stable (test FS) and unstable (test FU) limiting cases are shown in Figs. 2 and 3, respectively.

Table 3. Parameters for numerical tests under the f-plane approximation

	Stable case	Unstable case	Uncertain case	
	Test FS	Test FU	Test FC1	Test FC2
ζ_{yy}	8e–15	–8e–15	8e–15	–8e–15
ζ_{y0}	5.5e–10	–5.5e–10	5.5e–10	–5.5e–10
ζ_0	3e–5	–3e–5	[–1, –1.5, –2, –2.5, –3]e–5	[4, 3.5, 3, 2.5, 2]e–5

Table 4. Parameters for numerical tests under the β-plane approximation

	Stable case	Unstable case	Uncertain case		Threshold
	Test BS	Test BU	Test BC1	Test BC2	
ζ_{yy}	–8e–17	8e–17	–8e–17	8e–17	0
ζ_{y0}	4e–11	–4e–11	4e–11	–4e–11	8e–11
ζ_0	4.2e–5	–4.2e–5	[2.5, 2, 1, –2, –2.5]e–5	[–9, –6, –3, 0.5, 3]e–6	4e–5

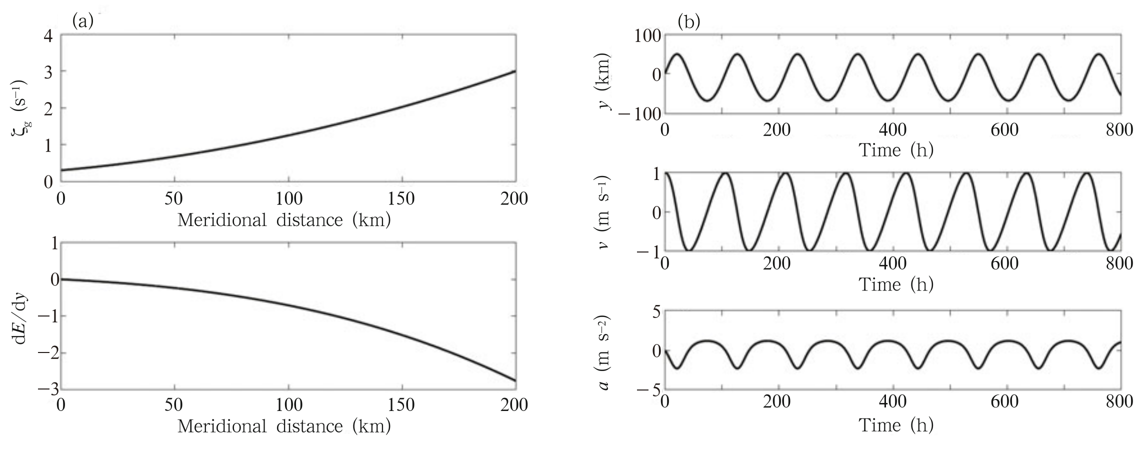

Fig. 2. (a) The meridional distributions of absolute vorticity (ζ_g; s^{-1}) and the meridional gradient of perturbation kinetic energy (dE/dy). (b) The time series of distance (y; km), velocity (v; m s^{-1}), and acceleration(a; m s^{-2}) for test FS.

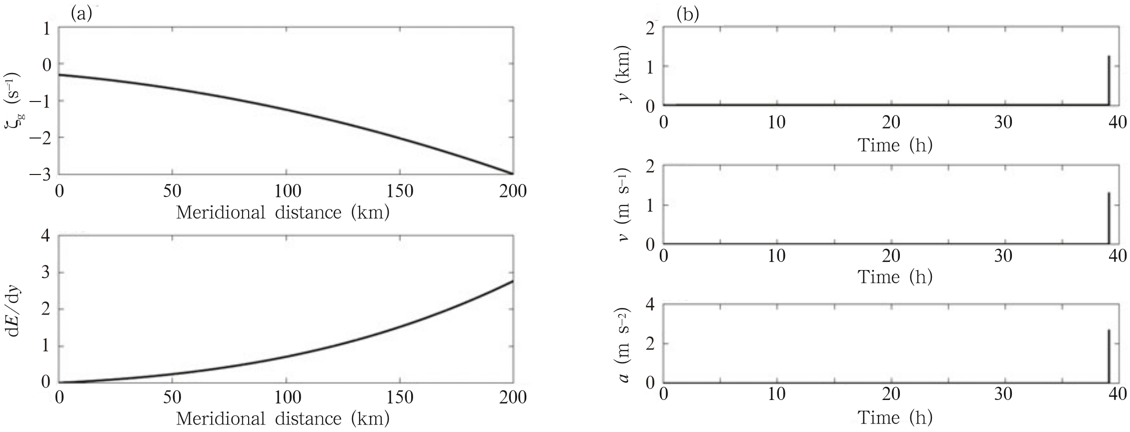

Fig. 3. As in Fig. 2, but for test FU.

The meridional gradient of perturbation kinetic energy $\mathrm{d}E/\mathrm{d}y$ decreases monotonically toward the north in the stable case (Fig. 2). Each of the variable time series follows a wave-like pattern with a period of approximately 100 h ($\sim$4 days). The time scale of these variations is consistent with the definition of inertial waves. The meridional displacement of the parcel is limited to approximately 100 km in either direction, and the magnitude of the perturbation velocity is systematically less than the initial value. The evolution of the acceleration nicely illustrates the effects of force variability on the motion. The fluctuations in the acceleration are weak and wave-like, and oriented in the opposite direction to the fluctuations in velocity. This result suggests that the force variability caused by the meridional variation of absolute vorticity acts as a restoring effect, generating an oscillation of the air parcel. By contrast, all of the variables increase dramatically with time in the unstable case (positive $\mathrm{d}E/\mathrm{d}y$). Test FS shows that a monotonic northward increase in $\zeta_{\rm g}$ results in stability, while test FU shows the monotonic decrease in $\zeta_{\rm g}$ results in instability. These results are consistent with the classical analysis of inertial instability.

The dynamic features of the system are more complicated if some of the criteria for the stable or unstable limiting cases are not satisfied. We have designed tests FC1 and FC2 to more fully explore these uncertain cases under the f-plane approximation. The parameters for these tests are listed in Table 3. We limit ourselves to varying the value of ζ_0 and investigate how these cases differ from the stable and unstable limiting cases. Each test comprises five members with different values of ζ_0.

The meridional distributions of $\zeta_{\rm g}$ and $\mathrm{d}E/\mathrm{d}y$ in test FC1 (Fig. 4a) are nearly identical to those in test FS (Fig. 2a), except that the sign of $\zeta_{\rm g}$ is different at the initial position. However, the time series of the variables have two new properties (Fig. 4b). First, the wave-like structure of the time series shows evidence of multiple periods. In particular, the acceleration spikes over a relatively short time in each cycle. This rapid growth in the acceleration is one order of magnitude greater than the normal growth over such a short time ($\sim$10 h), and implies a rapid intensification in the force acting on the air parcel. This intensification corresponds to a fast transition in the velocity from the negative extreme to the positive peak. The largest southward displacement is nearly 400 km. The rapid intensification of the force significantly influences the parcel trajectory and the direction of motion.

Second, the period of each time series changes with every cycle. One of the fundamental characteristics of chaotic systems is their sensitivity to initial conditions, which can be represented by the divergence of adjacent orbits in the phase plane. If the period of every cycle is constant, a trajectory in the phase plane circulates along a fixed orbit (as it does in the stable case). If the period changes with every cycle (as in Fig. 4b), the trajectories diverge into chaos with increasing iterations in the phase plane (Fig. 5) no matter how close the two orbits are initially.

The ensemble members in test FC2 transition from stability to instability with decreasing ζ_0. Figure 6 shows that a smaller value of ζ_0 corresponds to a smaller meridional region with $\mathrm{d}E/\mathrm{d}y < 0$, and therefore a greater likelihood of instability. Accordingly, the first two members (denoted by black and red lines in Fig. 7) have fixed orbits in the phase plane, while the other three members exhibit unstable behavior.

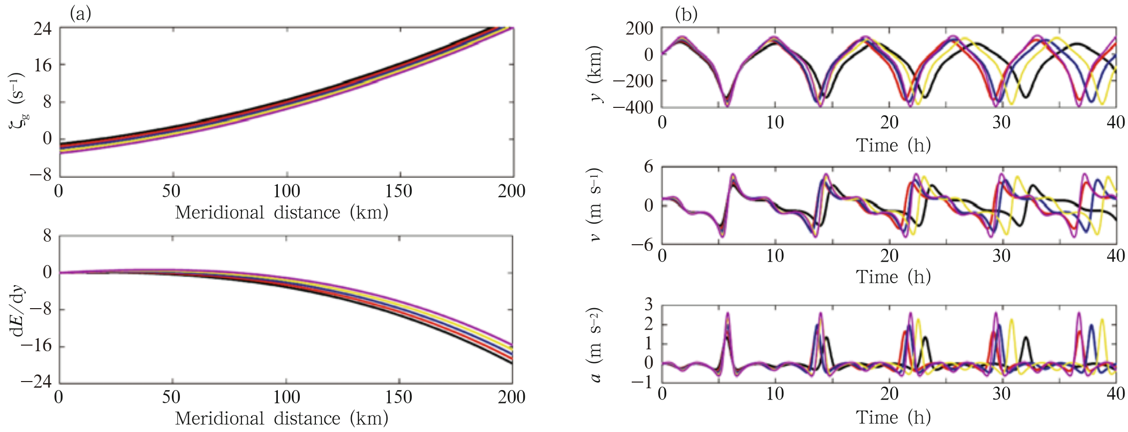

Fig. 4. As in Fig. 2, but for test FC1. The colors correspond to ζ_0 = –1×10^{-5} s^{-1} (black), ζ_0 = –1.5×10^{-5} s^{-1} (red), ζ_0 = –2×10^{-5} s^{-1} (blue), ζ_0 = –2.5×10^{-5} s^{-1} (yellow), and ζ_0 = –3×10^{-5} s^{-1} (violet).

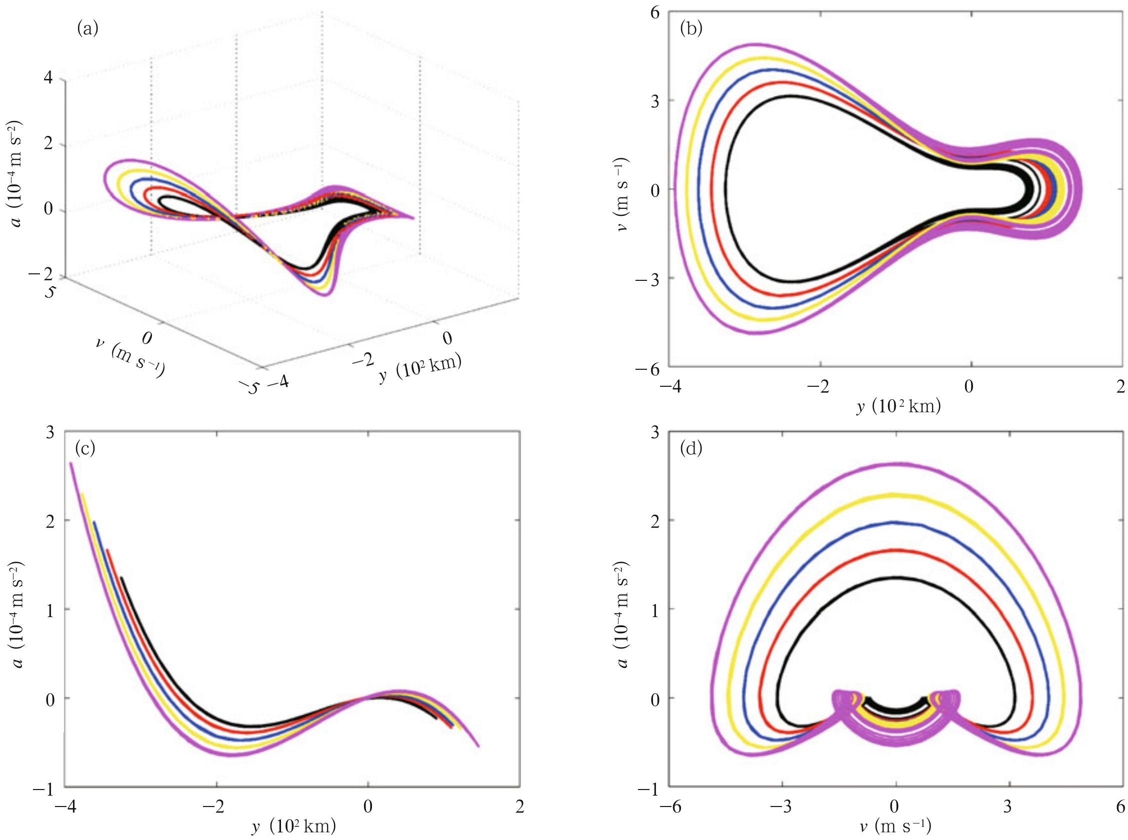

Fig. 5. Trajectories of perturbation distance (y; km), velocity (v; m s^{-1}), and acceleration (a; m s^{-2}) in (a) three dimensions, (b) the $y-v$ phase plane, (c) the $y-a$ phase plane, and (d) the $v-a$ phase plane for test FC1. The colors are the same as in Fig. 4.

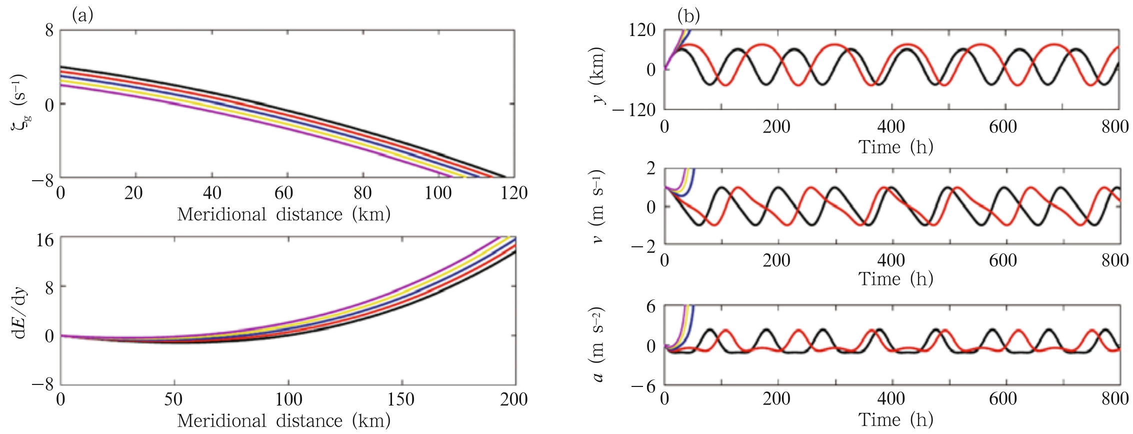

Fig. 6. As in Fig. 2, but for test FC2. The colors correspond to $\zeta_0 = 4\times10^{-5}$ s^{-1} (black), $\zeta_0 = 3.5\times10^{-5}$ s^{-1} (red), $\zeta_0 = 3\times10^{-5}$ s^{-1} (blue), $\zeta_0 = 2.5\times10^{-5}$ s^{-1} (yellow), and $\zeta_0 = 2\times10^{-5}$ s^{-1} (violet).

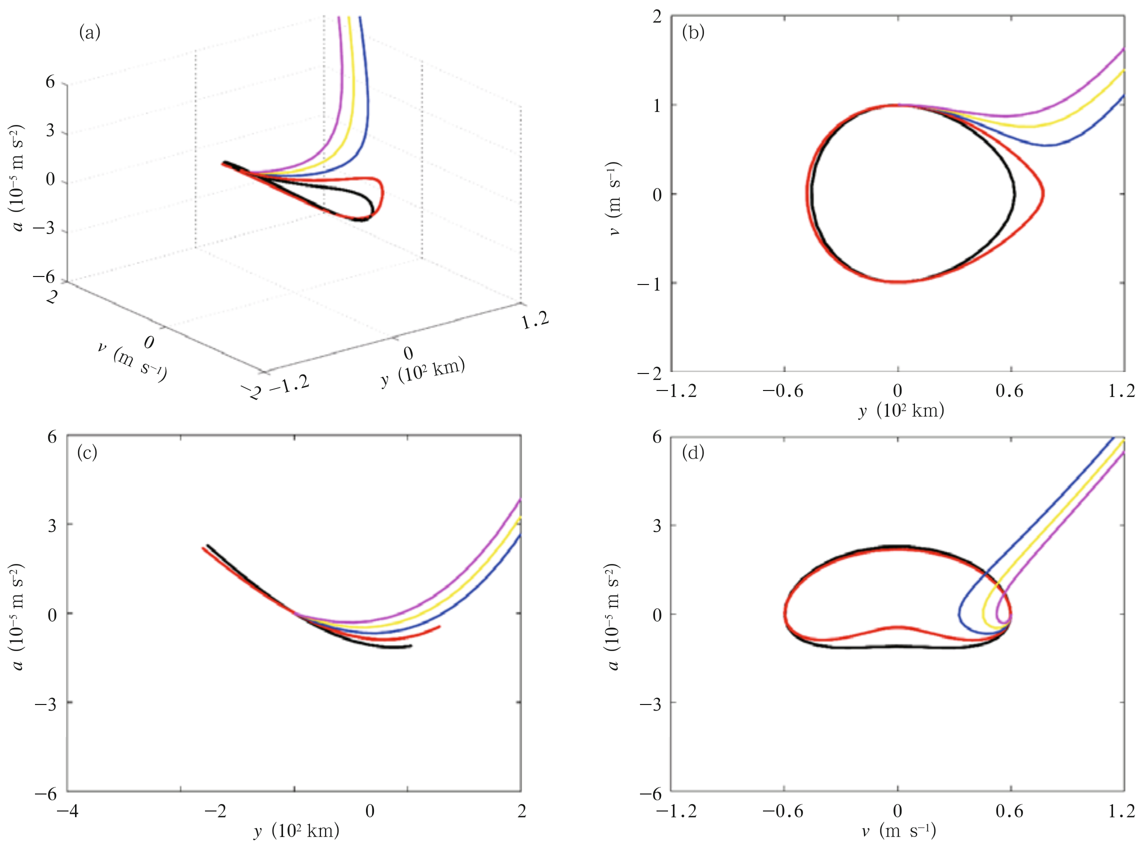

Fig. 7. As in Fig. 5, but for test FC2. The colors are the same as in Fig. 6.

The β-plane approximation is more appropriate than the f-plane approximation for large-scale motion. The parameters for these tests (Table 4) are therefore one or two orders of magnitude smaller than those used for the previous tests (Table 3). These parameters are specified to ensure that the range of variability in ζ_g is reasonable over a scale of 2000 km (Figs. 8a and 10a). The stable and unstable limiting cases under the β-plane approximation (tests BS and BU) produce patterns similar to those presented above (tests FS and

FU, respectively), and are omitted here.

The results of test BC1 are shown in Figs. 8 and 9. Disturbing ζ_0 from its stable configuration (i.e., test BS) results in an inverse state of inertial motion because the term $(1-\mathrm{e}^{\gamma y})$ in Eq. (20b) changes sign. The meridional variation in this term is more significant than the meridional variation in either of the other two terms. The time series of the variables (Fig. 8b) and their trajectories in phase space (Fig. 9) indicate that the system transitions from stable to unstable with larger perturbations to ζ_0.

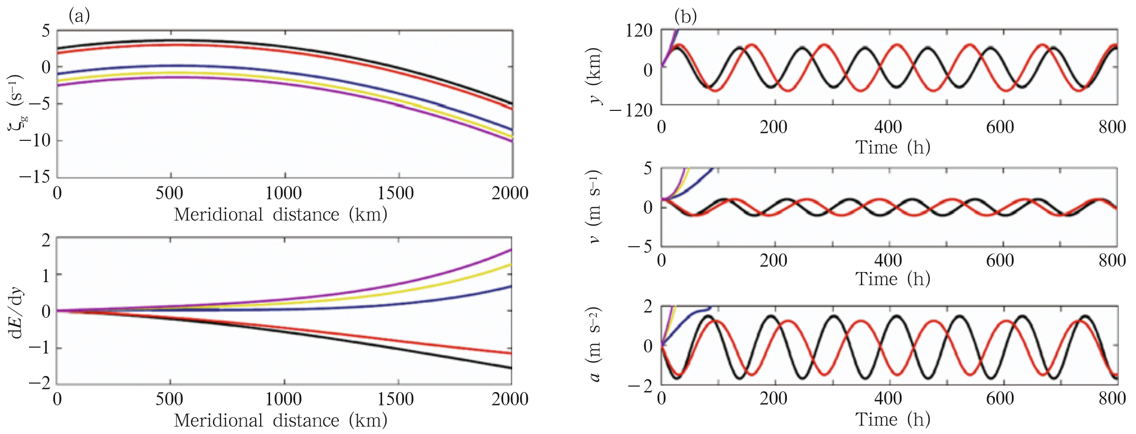

Fig. 8. As in Fig. 2, but for test BC1. The colors correspond to $\zeta_0 = 2.5\times10^{-5}$ s^{-1} (black), $\zeta_0 = 2\times10^{-5}$ s^{-1} (red), $\zeta_0 = 1\times10^{-5}$ s^{-1} (blue), $\zeta_0 = -2\times10^{-5}$ s^{-1} (yellow), and $\zeta_0 = -2.5\times10^{-5}$ s^{-1} (violet).

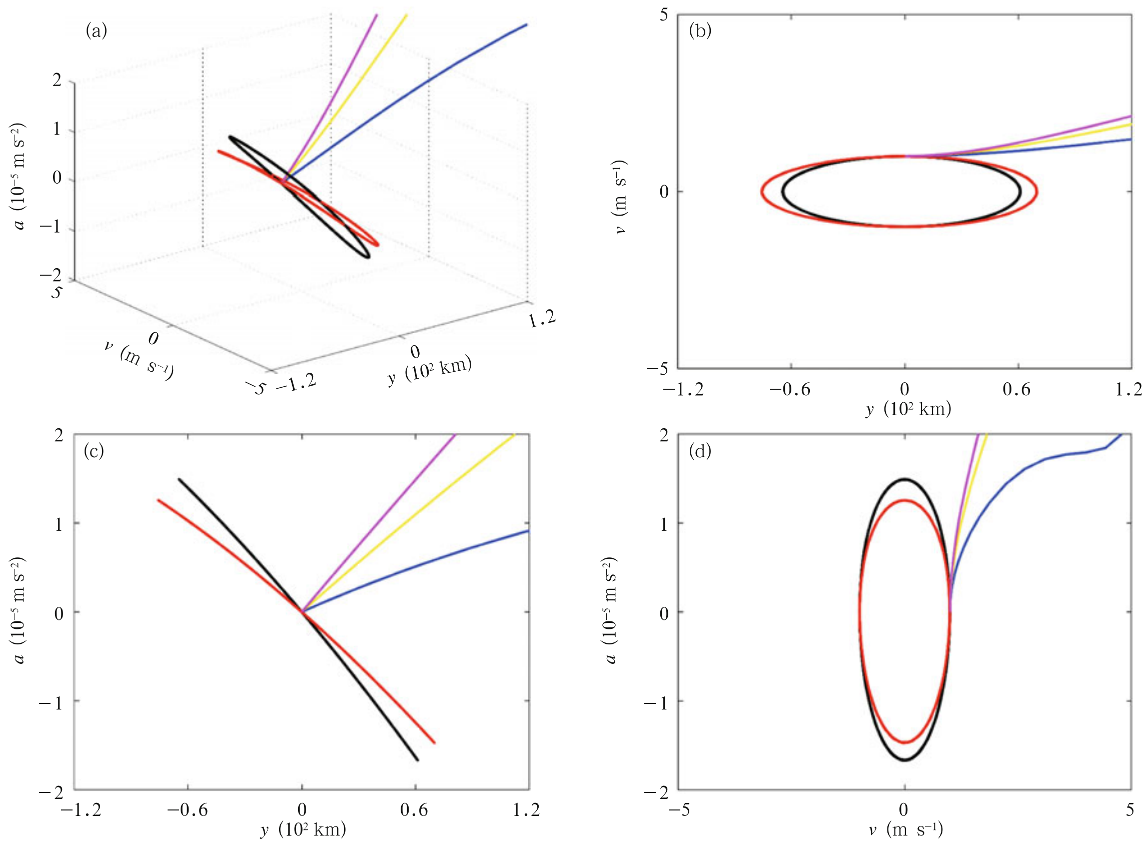

Fig. 9. As in Fig. 5, but for test BC1. The colors are the same as in Fig. 8.

Disturbing ζ_0 from its unstable limiting configuration yields chaotic behavior (test BC2). The time series in Fig. 10b suggest that the ranges of variability in all three variables are one order of magnitude larger than those in the f-plane approximation. Moreover, their rates of periodic change are faster than those in Fig. 4b. The trajectories of the individual ensemble members in phase space clearly diverge from one orbit to the next (Fig. 11).

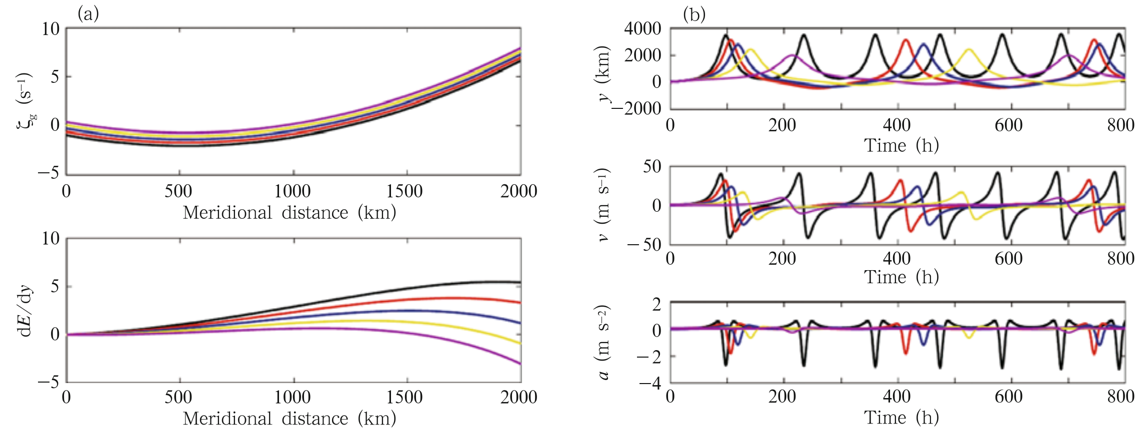

Fig. 10. As in Fig. 2, but for test BC2. The colors correspond to $\zeta_0 = -9\times10^{-5}$ s^{-1} (black), $\zeta_0 = -6\times10^{-5}$ s^{-1} (red), $\zeta_0 = -3\times10^{-5}$ s^{-1} (blue), $\zeta_0 = 0.5\times10^{-5}$ s^{-1} (yellow), and $\zeta_0 = 3\times10^{-5}$ s^{-1} (violet).

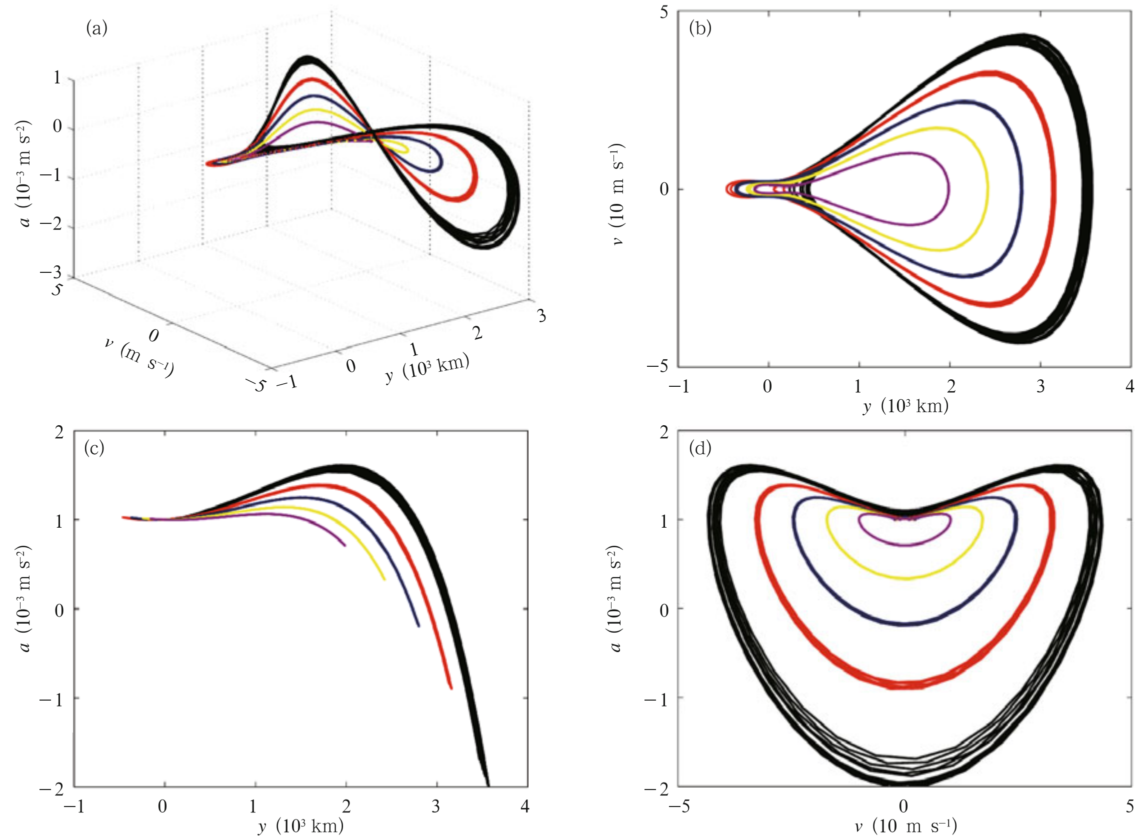

Fig. 11. As in Fig. 5, but for test BC2. The colors are the same as in Fig. 10.

5. Summary

Newtonian jerky dynamics are used to investigate the dynamical features of inertial instability associated with meridional variations of absolute and planetary vorticity. The results reveal interesting properties of the motion that differ from those identified using classical inertial instability analysis.

Theoretical analysis of the Newtonian jerky dynamics reveals that the criteria for inertial instability are fundamentally tied to the value of $\mathrm{d}E/\mathrm{d}y$, which is dependent on the meridional distributions of absolute vorticity (ζ_{g}) and planetary vorticity (the β effect). The meridional structure of ζ_{g} is a key factor in determining the dynamical features of the flow. The criteria for stability or instability under the f-plane approximation depend not only on the meridional distribution of ζ_{g}, but also on the values of ζ_y and ζ_{g} at the initial position. These characteristics of the flow can be represented by the structural parameters ζ_{yy}, ζ_{y0}, and ζ_0. Accounting for the β effect introduces an explicit nonlinear term ($y'y''$). This nonlinear term does not alter the instability criteria or the dynamical features of inertial motion in the constant ζ_{g} case; however, it exerts a significant influence on the instability criteria if ζ_{g} varies in the meridional direction. The required value of ζ_{yy} for stability (or instability) changes signs, and the threshold values of ζ_{y0} and ζ_0 become substantially more complicated ($|\zeta_{yy}|/\gamma$ and $|\gamma\zeta_{y0}+\zeta_{yy}|/\gamma^2$, respectively).

We have presented a numerical analysis of the time series of position, velocity, and acceleration associated with different values of the structural and Coriolis parameters, as well as the trajectories of these variables in the phase plane. Smooth changes in acceleration correspond to steady wave-like variations in position and velocity. By contrast, intensely varying forces and associated rapid changes in acceleration lead to track shifts and abrupt changes in direction. The stable limiting cases under the f- and β-plane approximations exhibit periodic wave-like behavior, while the unstable limiting cases correspond to exponential growth. We have perturbed the value of ζ_0 to explore the uncertain territory between these two limiting cases. Small perturbations to the value of ζ_0 may lead not only to inversion of the stability (or instability) of the flow, but also to the emergence of chaos. This result implies limits to the predictability of inertial motion in such cases.

We have introduced Newtonian jerky dynamics via a simple application to inertial instability. Newtonian jerky dynamics is an effective framework for studying the dynamical features of atmospheric motion. This framework explicitly considers both nonlinear terms and the physical meaning of force, and therefore represents a useful tool for furthering our understanding of atmospheric evolution under the action of intensely varying forces.

Acknowledgments. The language editor for this manuscript is Dr. Jonathon S. Wright.

REFERENCES

Dutton, J. A., 1995: *Dynamics of Atmospheric Motion*. Dover Publications Inc., New York, 298–301.

Emanuel, K. A., 1979: Inertial instability and mesoscale convective systems. Part I: Linear theory of inertial instability in rotating viscous fluids. *J. Atmos. Sci.*, **36**(12), 2425–2449.

——, 1982: Inertial instability and mesoscale convective systems. Part II: Symmetric CISK in a baroclinic flow. *J. Atmos. Sci.*, **39**(5), 1080–1097.

French, A. P., 1971: *Newtonian Mechanics*. W W Norton & Co, New York, 170–173.

Gottlieb, H. P. W., 1996: Question 38: What is the simplest jerk function that gives chaos? *Am. J. Phys.*, **64**(5), 525.

——, 1998: Simple nonlinear jerk functions with periodic solutions. *Am. J. Phys.*, **66**(10), 903–906.

Huang Peitian, 1981: Jerk–A new concept to describe the mechanical motion. *Physics*, **10**(7), 394–397. (in Chinese) (http://www.wuli.ac.cn/CN/abstract/abstract27243.shtml)

Linz, S. J., 1997: Nonlinear dynamical models and jerky motion. *Am. J. Phys.*, **65**(6), 523–526.

——, 1998: Newtonian jerky dynamics: Some general properties. *Am. J. Phys.*, **66**(12), 1109–1114.

Lorenz, E. N., 1963: Deterministic nonperiodic flow. *J. Atmos. Sci.*, **20**(2), 130–141.

Mei Fengxiang, Liu Duan, and Luo Yong, 1991: *Advanced Analytical Mechanics*. Beijing Institute of Technology Press, Beijing, 194–249. (in Chinese)

Montgomery, M. T., and R. J. Kallenbach, 1997: A theory for vortex Rossby waves and its application to spiral bands and intensity changes in hurricanes. *Quart. J. Roy. Meteor. Soc.*, **123**(538), 435–465.

Rayleigh, L., 1916: On the dynamics of revolving fluids. *Prof. Roy. Soc. London.*, **A93**, 148–154.

Rozoff, C. M., D. S. Nolan, J. P. Kossin, et al., 2012: The roles of an expanding wind field and inertial stability in tropical cyclone secondary eyewall formation. *J. Atmos. Sci.*, **69**(9), 2621–2643.

Saltzman, B., 1962: Finite amplitude free convection as an initial value problem–I. *J. Atmos. Sci.*, **19**(4), 329–341.

Schubert, W. H., and J. J. Hack, 1982: Inertial stability and tropical cyclone development. *J. Atmos. Sci.*, **39**(8), 1687–1697.

Schot, S. H., 1978: Jerk: The time rate of change of acceleration. *Am. J. Phys.*, **46**(11), 1090–1094.

Sprott, J. C., 1997a: Some simple chaotic flows. *Phys. Rev. E*, **50**(2), E647–E650.

——, 1997b: Some simple chaotic jerk functions. *Am. J. Phys.*, **65**(6), 537–543.

Tomas, R. A., and P. J. Webster, 1997: The role of inertial instability in determining the location and strength of near-equatorial convection. *Quart. J. Roy. Meteor. Soc.*, **123**(542), 1445–1482.